View metadata, citation and similar papers at core.ac.uk

brought to you by CORE

provided by IntechOpen

We are IntechOpen, the world's leading publisher of Open Access books Built by scientists, for scientists

4,800
Open access books available

122,000
International authors and editors

135M
Downloads

Our authors are among the

154
Countries delivered to

TOP 1%
most cited scientists

12.2%
Contributors from top 500 universities

CLARIVATE ANALYTICS BOOK CITATION INDEX INDEXED

WEB OF SCIENCE™

Selection of our books indexed in the Book Citation Index in Web of Science™ Core Collection (BKCI)

Interested in publishing with us?
Contact book.department@intechopen.com

Numbers displayed above are based on latest data collected.
For more information visit www.intechopen.com

6

Wearable Energy Harvesting System for Powering Wireless Devices

Yen Kheng Tan and Wee Song Koh
Energy Research Institute @ NTU (ERI@N)
Singapore

1. Introduction

As the world trends towards ageing population UN (2011), there is an increasing demand and interest in using technology to increase the quality of life for elderly people. An expanding area of interest is heading towards the health care applications like wearable biometric monitoring sensors. These monitoring nodes, typically powered by batteries, have various functions like sensing & monitoring bodily functions, after which the data is wirelessly transmitted to a remote data terminal Harry et al. (2009), Philippe et al. (2009). However such applications mentioned are not new, where earlier literatures envisioned of a not too distant future where e-textiles, electronics woven together with fabrics, are omni-present Marculescu et al. (2003). With improving technology in miniaturization and wireless communication, clothing containing sensors for sensing and monitoring bodily physiological functions Wixted et al. (2007) is becoming more common and widespread. Such devices should be unobtrusive wearable, flexible, lightweight and ideally self-sufficient.

In using batteries, the useful life of a wearable sensing device Cook et al. (2004) is usually limited by the battery's lifespan or capacity. Using a high energy capacity AA sized battery of 3000mAh, the life of battery powering a certain sensor node can last a maximum of 1.5 years Kheng et al. (2010). But operation life of the wearable electronic is much longer, at least several years. Therefore its normal operation will be interrupted whenever the supplying batteries die out. Typically, the higher the capacity of the battery, bigger in size the battery will be. With miniaturization, device components like sensors, accompanying electronics and board size will shrink and get smaller. As such, wearable flexible batteries are more commonly used to replace the larger batteries to keep pace with the shrinkage of these wearable electronics. But capacity of a flexible thin-film battery with a volumetric size of 1.2 cm^3 is about 30 mAh, lower than a 2850mAh capacity AA alkaline battery of volumetric size 11 cm^3. As a result, sustainability is often a key challenge for systems to be standalone with 'Deploy & Forget' feature.

The addition of energy harvesting source is identified as a feasible way to increase the device's operation duration. Several potential ambient energy sources are discussed, with the photovoltaic (PV) harvesting method providing the highest power density per volume of total system Raghunathan et al. (2005). For indoor application using PV harvesting, major challenges include: poor lighting intensity as compared to outdoor lighting intensity; limited sized PV panel to be used if the device is to be placed in a confined area of the human body. Such power produced by the PV panel is very small, usually in the range of hundreds of

μW. Indoor light intensity in office environment is in the range of < 10 W/m^2, compare with 100-1000 W/m^2 for outdoor conditions Hande et al. (2007). For photovoltaic panel, amorphous type is the best suited for indoor applications but suffers from low efficiency, in the range of 3% - 7% Randall et al. (2002). On the other hand, PV cells provide a fairly stable DC voltage through much of their operating space Roundy et al. (2004). Various works utilizing solar harvesting/scavenging techniques demonstrated the suitable of indoor PV in supplying alternate energy to small, low-power consuming devices, complemented with batteries within the system Hande et al. (2007), Nasiri et al. (2009).

In this chapter, a flexible and self-sustainable energy solution incorporating energy harvesting for wearable electronics is presented. Introducing of energy harvesting technique levitate the operation of system towards self-sustainability. However for the system to be wearable, certain amount of device flexibility or bending is needed. Generally the device should not be rigid, not inhibit motion in any way and ideally follow as closely to the contour of the wearer's body. As such, in this chapter, rigid batteries like the AA size battery, PV panel, PCB and supercapacitor are replaced with the flexible, bendable version. Capacity of a typical flexible battery is in the range of a few tens of mAh Hahn et al. (1999), which severely restrict the node's operation duration if the flexible battery is the only input source. As such, an additional input source is hybrid with the primary battery (which in this case, PV panel is chosen as the additional input source to complement the primary battery for powering the wireless body sensors). Flexible super capacitors with capacitance of $\approx$ 11 F/g has been realized with good capacitance stability for long term usage applications Gan et al. (2009). The rest of the chapter is organized as follows: Section II introduces the wearable energy storage for wireless body sensor network and section III illustrates in more details about the key part of the proposed system: flexible energy harvesting system comprising of modules like maximum power point tracking (MPPT), current limiter, voltage regulation within the power management circuitry and the load requirements. After which, in section IV, the hybrid of wearable energy storage and FEH is discussed. Experimental results of the proposed system performance are illustrated in section V and conclude the chapter with section VI.

2. Wearable energy storage for wireless body sensor network

It is anticipated that people will soon be able to carry a personal body sensor network (WBSN) system with them that will provide users with information and various reporting capabilities for medical, lifestyle, assisted living, sports or entertainment purposes. In the literature, some older medical monitoring systems (such as Holter monitors) record the hosts' data for off-line processing and analysis. Newer wearable wireless systems provide almost instantaneous information that help in earlier detection of abnormal conditions. There are also many such commercial products out there to allow wearers to monitor their vital signs, for examples, Omron health care products like blood pressure meter, thermometer and portable ECG and Philips vital sense product and sports monitoring devices as seen in Figures.1 and 2. For these commercially available health care products as seen in Figure.1, although they are meant to be made for small size and portable, in actual fact, they are too big and bulky to be integrated as part of our bodies for monitoring. Part of the reason why these products are so huge is because of the batteries. Moreover, these products operate heavily on their onboard batteries and if they are to conduct continuous body monitoring, their operational lifetimes are very short, a month or even less than that.

Fig. 1. Omron healthcare products (a) portable ECG, (b) thermometer and (c) blood pressure meter and Philips product (d) vital sense device

Fig. 2. Body worn devices for measuring activity and energy expenditure

Having said that, these body worn devices are still receiving huge attentions and commercial demands simply because of their outstanding features, but they really need to be highly portable and easily embeddable into our bodies for monitoring. In addition to that, the catch with these body worn devices is the sky high prices to own an outstanding system like this, i.e. a few hundreds or even to a thousand dollars. If there are a few more places on the human body for close measuring and monitoring of dedicated activities like sleeping, sporting, etc., it will cost a huge sum to implement the body monitoring system. There is no doubt about the potential of such body worn monitoring system and the market is huge demanding for such distributed sensing of human well beings through their vital signs. However, the present state of arts and commercial products are limited and there are more to what they have that could be included. As compared to the conventional large and bulky body monitoring system mentioned earlier, the availability of microelectronics devices and micro electromechanical systems (MEMS) like pulse oximeters, accelerometers, energy harvesting devices, etc. Wixted et al. (2007), Cook et al. (2004) integrated with wireless technology provides an alternative, non-invasive, distributed and self-powered method of automatic monitoring activity. In addition, many of such miniaturized electronic devices are integrated together into each individual person and also into their activities to enable better human-computer interaction to achieve all-rounded monitoring of human health lifestyle and more accurate performance assessment of the athletes as illustrated in Figure.3.

The functionality of the proposed body monitoring system in Figure.3 on each individual human being is illustrated as follows: the sensed physiological information of the human is stored and accumulated in the memory of the sub-GHz ultra-wide-band (UWB) transmitter and it is periodically communicated to the UWB receiver of the base station without mutual interference. One of the approaches is by coding the sequence or using different time slots, the receiver can identify the transmitter from which sensor and setup the link automatically. The received data from various smart sensors deployed around the body are then used for performance assessment of subject under test. Wireless communication does away the wires, hence save the wearer of this proposed body monitoring system from the phobia of wires.

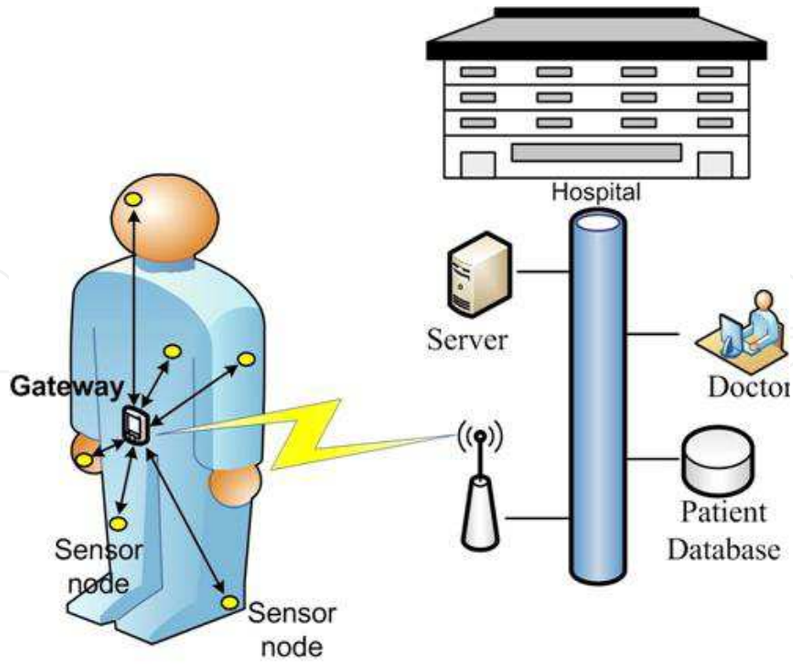

Fig. 3. Human health lifestyle monitoring

Even though wires are removed, battery becomes the concern as the operational lifetime of the energy storage is limited. The effective duration of a battery driven body monitoring system is short in terms of days of weeks, after which the monitoring purpose is gone.

The energy problem escalates further when there is a need for the energy storage to be flexible and wearable, able to conform to human body. According to the authors of Harry et al. (2009) and Philippe et al. (2009), both suggested the use of thin-film battery technology to shrink the overall package size, where lithium polymer battery sizes of 85 mm x 55 mm x 0.5 mm and 59 mm x 35 mm x 0.5 mm (PGEB0053559) to achieve the wearable energy storages. Typical flexible (thin film solid state) batteries are constructed by depositing the components of the battery as thin films (usually in tens of μm) on a substrate, which includes a solid substrate of electrolyte cathode (positive electrode) and anode (negative electrode). Advantages include small physical size, able to be used in a very broad range of temperatures, and supposedly more eco-friendly than conventional batteries Mcdonald (2011). However, as with all batteries applied on WBSN, they will be drained off after a certain period of time. In Harry et al. (2009) and Philippe et al. (2009), rechargeable lithium polymer battery capacity is of 50 to 200 mAh (12 hours to 50 hours of operation) and 65 mAh at 3.7 V respectively. Clearly, wearable energy storage alone is not able to sustain the operation of the WBSN. There is a need to seek for a supplement flexible energy harvesting system to prolong the operational lifetime of the WBSN.

3. Flexbile energy harvesting system

To minimize the problem associated with batteries, using of photovoltaic as an addition energy source is proposed as a solution to complement battery (Zn-MnO_2 flexible battery

Barbic et al. (1999), rated voltage at about 1.5 V and capacity of ≈ 30 mAh) in prototype and to prolong the operational life of the wearable device.

3.1 Characteristics of PV panel

Photovoltaic cell converts light to electricity through a physical process called the photovoltaic effect. Light (in the form of photons) that is absorbed into the PV cell will transfer its energy to the semiconductor device, knocking electrons loose and allowing them to flow freely. These generated electrons are transferred between different bands (example, from the valence to conduction bands) within the material, resulting in the buildup of voltage between two electrodes. Electrically, a solar cell is equivalent to a current generator in parallel with an asymmetric, non-linear resistive element (example: a diode). When illuminated, the ideal cell will produce a photocurrent proportional to the light intensity. That photocurrent is divided between the variable resistance of the diode and the load, in a ratio which depends on the resistance of the load and the level of illumination. For higher resistances, more of the photocurrent flows through the diode, resulting in a higher potential difference between the cell terminals but a smaller current though the load. The diode thus provides the photovoltage. Without the diode, there is nothing to drive the photocurrent through the load Nelson (2011).

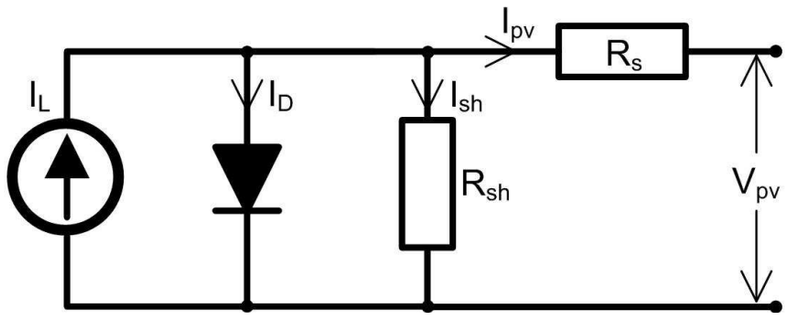

Fig. 4. Equivalent electrical circuit for a photovoltaic cell with parasite resistances

Figure.4 shows the basic equivalent circuit of a PV cell, where I_L - light-generated current, I_D - reverse saturation (dark) current of the PN diode, R_s - series resistance, R_{sh} - shunt resistance. Dark current can be viewed as caused by the potential built up over the load and flows in the opposite direction. When the shunt resistance, R_{sh} is assumed to be infinite, the current-voltage (I-V) characteristic of the photovoltaic (PV) module can be described with a single diode as the four-parameter model given by,

$$I_{pv} = I_L - I_D \left[exp\left(\frac{V_{pv} + I_{pv} R_s}{N_s n_I V_t} \right) - 1 \right] \tag{1}$$

where V_t - the junction terminal voltage, N_s is the number of cells in series and n_I is the diode ideality factor Celik (2007). For this prototype, off-the-shelf Sundance Solar MPT3.6-75 Sundance (2011) flexible PV panels, made up of amorphous silicon on a polymer substrate, is used. Dimensions are about 75 mm x 72 mm x 0.5 mm. PV characterization graphs are shown in Figures.5 and 6. At ≈ 400Lux, it is able to provide a peak power of about 0.14 mW.

Any unused energy will be stored into a flexible supercapacitor, which is ideal for energy storage that undergoes frequent charge and discharge cycles at high current and short

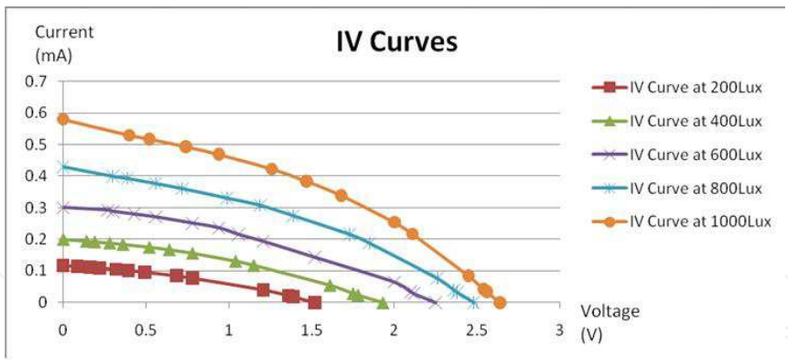

Fig. 5. IV Curves of PV panel at various Lux values

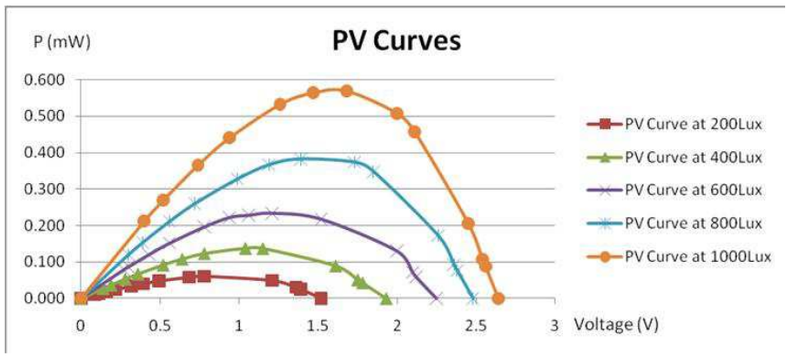

Fig. 6. PV Curves of PV panel at various Lux values

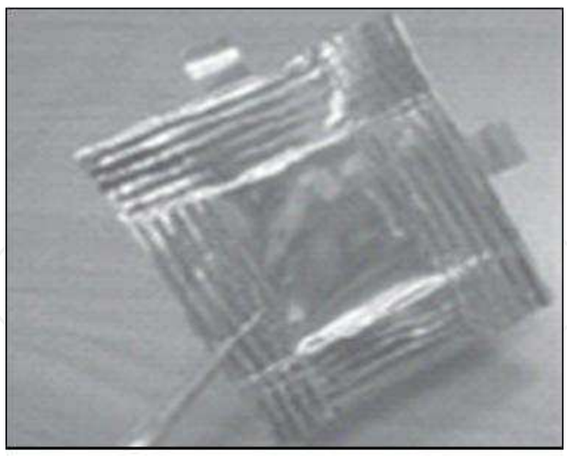

Fig. 7. A flexible supercapacitor laminated using polymer-coated aluminum foil

duration. Basically the plates of a supercapacitor are filled with two layers of the identical substance for separating the charge, instead of having dielectric, resulting in a much larger surface area and high capacitance. Experiments using various types of electrodes and electrolyte had been extensively carried out, like experimenting VNF electrodes in aqueous

electrolyte of different pH and also in an organic electrolyte Grace et al. (2010). Dimension of such flexible capacitors as shown in Figure.7 can be packaged to about the same size as the flexible battery.

3.2 Fractional open-circuit voltage MPPT technique

Maximum Power Point Tracking (MPPT) is a frequently used technique to vary the electrical operating point of the PV module so that the module is able to deliver its maximum available power. Various MPPT techniques are grouped into 'Direct' or 'Indirect' methods Salas et al. (2005). For indirect methods ("quasi seeks"), the Maximum Power Point (MPP) is estimated from the measures of the PV generator's voltage and current PV, the irradiance, or using empiric data, by mathematical expressions of numerical approximations. They do not obtain the maximum power for any irradiance or temperature and none of them are able to obtain the MPP exactly. But in many cases, such methods can be simple and inexpensive. The direct methods ("true seeking methods") obtain the actual maximum power from the measures of the PV generator's voltage and current PV. Although Fractional Open Circuit Voltage based MPPT method is classified as a quasi seeks method, it is also considered to be one of the simplest and cost effective method Masoum et al. (1999). It is based on the fact that the PV array voltage corresponding to the maximum power exhibits a linear dependence with respect to the array open circuit voltage for different irradiation and temperature levels. Maximum power point voltage, $V_{MPP} = K_{oc} * V_{oc}$, where V_{oc} is the open circuit voltage of the PV and K_{oc} is the voltage factor Ahmad (2010). To operate the PV panel at the MPP, the actual PV array voltage V_{pv} is compared with the reference voltage V_{ref} which corresponds to the V_{mpp}. The error signal is then processed to make $V_{pv} = V_{ref}$. Normally, the panel is disconnected from the load momentarily to sample its open circuit voltage. The fraction of the open circuit voltage corresponding to the V_{mpp} is measured and is kept in a hold circuit to function as V_{ref} for the control loop.

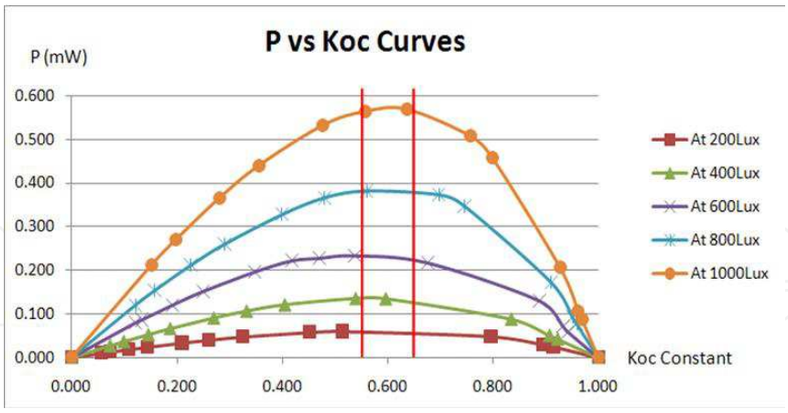

Fig. 8. Graph of Power vs Koc Constants

In Figure 8, the peak power of the PV panel is found between K_{oc} constant values of 0.55 to 0.65. The K_{oc} part of the control circuit will reference a K_{oc} constant of 0.65 to V_{oc} as V_{ref}. The control circuit will be built using discrete components and op-amps.

3.3 Ultra-low-power management circuit

The MPPT control circuitry block diagram is shown in Figure.9. It is designed to boost V_{pv} to the load when it has fallen below the V_{ref} reference value. First the PV panel will break open from rest of circuit by means of a switch. This open circuit voltage will be captured by the K_{oc} circuit, multiplied by the K_{oc} constant to become V_{ref}. After a certain time interval, the PV panel will connect back with the rest of the circuit. If $V_{pv} < V_{ref}$, the error signal will be amplified and compared with a sawtooth waveform, with the resultant signal controlling the gate of the DC-DC converter.

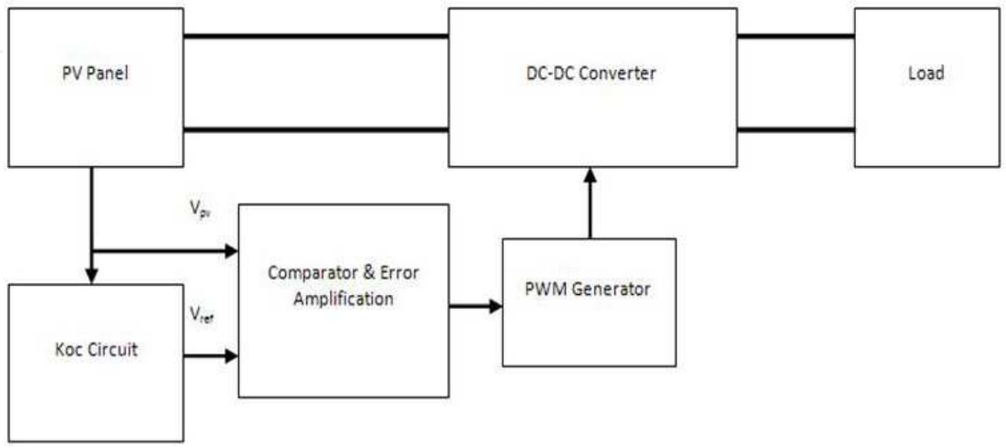

Fig. 9. Block diagram of the Fractional Open Circuit Voltage MPPT control circuit

Using discrete components to build this control circuit, MOSFET are used as switches where timing switching will be controlled by pre-programmed pulses from MSP430 MCU onboard the end device. Koc constant of 0.65 is obtained using voltage dividing in the Koc circuit. Op-amps, capacitors, resistors and Schottky diodes are used in various part of the circuit for comparisons and simple sample & hold operations.

3.4 Wireless body sensor nodes/network

The wireless body sensor node is developed from the target board from Texas Instruments eZ430-RF2500 Development Tool Texas Instruments (2011), which measures the body temperature of the wearer and communicates wirelessly to an access point connected to a PC. It operates between 1.8 V to 3.6 V, and measured 35 mm x 20 mm x 3.5 mm, which can be easily placed into cloths pocket or between layers of sewn clothing. The communication profile is captured in Figure.10.

Referring to Figure.10, during the sleep/standby mode, the target board consumes around 1.2 μA of quiescent current. During initialize stage, instantaneous current can rise up to about 20 mA and 2 mA for burst mode transmission, which is taken care of by the flexible supercapacitor. To reduce current consumption by the load, the target board had been configured to transmit data at a $\approx$ 5 seconds transmission period. In its original mode, its average current consumption over 1 second transmission period is 36.80 μA Texas Instruments (2011).

$$I_{ave} = [I_{sleep} + I_{Tx,Total}]/T_{Tx} \quad (2)$$

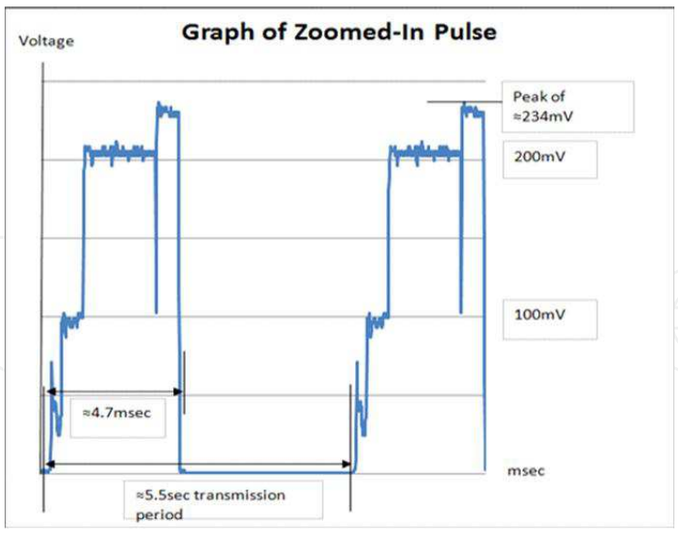

Fig. 10. Zoomed-In pulse current consumption by the TI Target Board with modified configuration of ≈ 5 second transmission period. Graph captured across a 10Ω current sensing resistor in series with load

where

$$\begin{aligned} I_{sleep} &= [I_{idle}(MSP430) + I_{idle}(CC2500)] * [T_{Tx}(sec) - T_{app}(sec)] \\ &= 1.3[\mu A] * (1[s] - 2.838[ms]) \\ &= 1.296A * s \end{aligned} \tag{3}$$

Therefore average current consumption over 1 second transmission period: I_{ave} (1 sec Tx period) = (1.296 [μA*s] + 35.508 [μA*s]) / 1 [s] = 36.80 μA. If transmission period is extended to ∼5 second, the sleep current: I_{sleep} (over 5 sec Tx period) = 1.3 [ţA] * (5 [s] - 2.838 [ms]) = 6.496 μA*s and the average current consumption over 1 second: I_{ave} (over 1 sec for a 5sec Tx period) = (6.496 [μA*s] + 35.508 [μA*s]) / 5 [s] = 8.4 μA

Therefore the less frequently the target board transmits, the less average current is consumed.

If using battery of 1000 mAh capacity for average current of 36.80 μA consumption, calculated life expectancy = 1000 [mA*hrs] / 0.0368 [mA] ≈ 3.10 years. If using battery of 30 mAh capacity for average current of 36.80 μA consumption, calculated life expectancy = 30 [mA*hrs] / 0.03680 [mA] ≈ 33.97 days. If using battery of 30mAh capacity for average current of 8.4 μA consumption, calculated life expectancy = 30 [mA*hrs] / 0.0084 [mA] ≈ 148.8 days.

Such calculations constitute an perfect scenario, where there is no leakages, 100 % efficiency, no power loss, no surges, and can only be used as a rough guide in the calculation of the life expectancy of battery of certain capacity, and the actual current consumption of the node. In the worst case scenario, the end device will keep initializing when scanning to linkup with the access point, which will continuously draw about 18 mA of current.

4. Hybrid flexible energy harvesting and energy storage

The proposed hybrid flexible energy system prototype as seen in Figure.11 incorporate three different types of energy sources, mainly the primary battery (flexible batteries), the secondary battery (flexible supercapacitor, which acts as energy storage) as well as renewal energy harvesting source like the flexible PV panel (Additional input energy to complement primary batteries) to harvest ambient light energy.

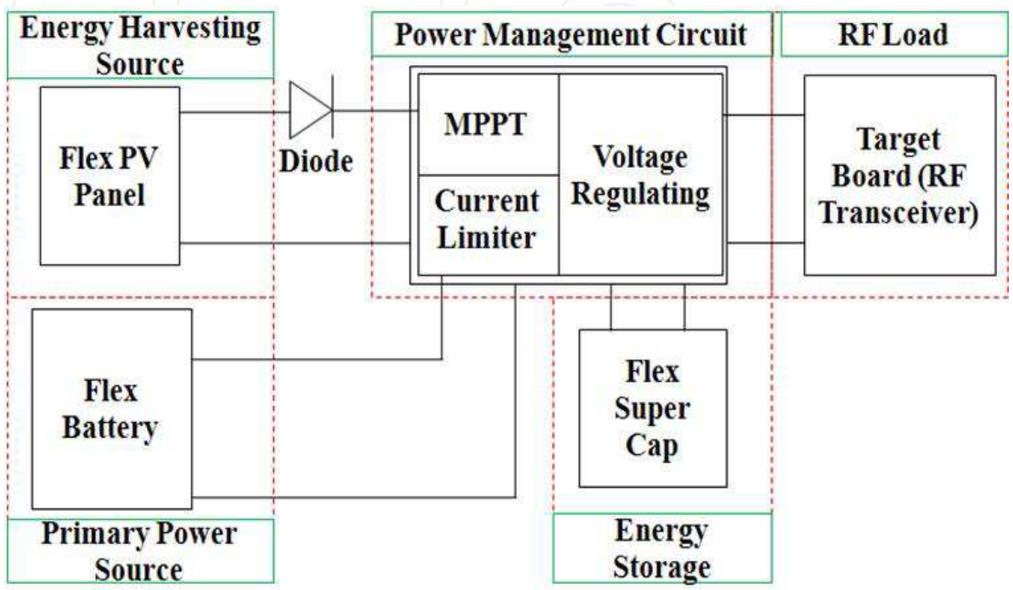

Fig. 11. Block diagram of the proposed hybrid energy harvesting and storage system

The RF transceiver load typically has 2 modes of operation: sleep and transmission. In sleep mode, it consumes around 1.2 μA of quiescent current, and in transmission mode, it consumes around 2 mA of current. The default transceiver setting is set at 1 transmission for every 1 second period. During sleep mode, the transceiver consumes very little energy, where excess unused energy from the primary battery and PV panel will be stored in the flexible supercapacitor. During transmission mode, the transceiver will draw energy mainly from the supercapacitor, which is able to manage the sudden current surge. Subsequently, the transceiver goes into sleep mode and the supercapacitor starts to recharge from the primary battery and PV panel. To conserve energy, period between transmissions is increasing, which decrease energy usage and increase the charging time for supercapacitor.

The overall system design of the proposed hybrid flexible energy harvesting and storage solution is illustrated in Figure.11. The power management circuitry of the system depicted in Figure.11 consists of: MPPT control, flexible battery current limiter and a load voltage regulator, to be fabricated onto a flexible PCB substrate. MPPT control provides a simple mean of impedance matching between PV panels to load. The current limiter protects the primary battery from sudden surges. Voltage regulator maintains a steady voltage level as required by the transceiver load. Referring to Figure.12, the MPPT control circuit is designed to boost V_{pv} to the load when it has fallen below the V_{ref} value. To capture the open circuit voltage of the PV panel, NMOS 1 will be opened to isolate the PV panel from rest of the circuit,

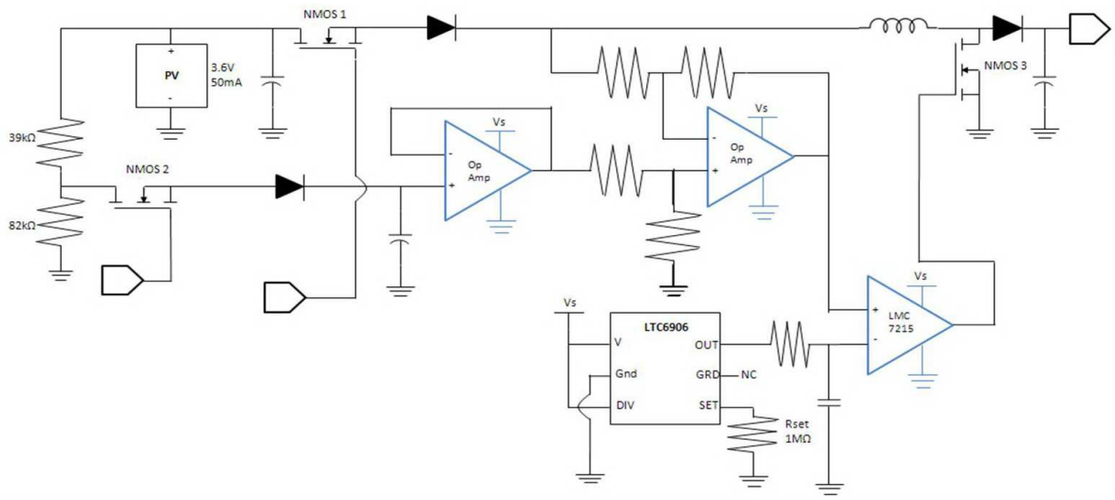

Fig. 12. MPPT Control Circuit using Fractional Open Circuit Voltage Approach

while NMOS 2 will be closed. The open circuit voltage will be acquired by the K_{oc} circuit, which is a voltage dividing circuit, and multiplied by the predetermined K_{oc} constant of 0.65 to become V_{ref}. Subsequently this V_{ref} value is stored by an op amp sample and hold circuit. Pre-programmed timers signal from MSP430 MCU onboard the TI end device will provide the switching timing for NMOS 1 and NMOS 2. After a set timing, NMOS 2 will be opened whereas NMOS 1 will be closed. The voltage from the PV panel, V_{pv}, will be compared with the V_{ref} at the second op amp, which is a differential amplifier. When V_{pv} is lower than V_{ref}, a voltage output will be sent to the '+' input of the LMC7215 comparator, which will compare with the sawtooth waveform from LTC6906. This will provide switching for NMOS 3 of the boost converter.

5. Experimental results

5.1 Performance of flexible energy harvesting system with MPPT scheme

In switching the gate of NMOS 3, there must be output from LMC7215, meaning the sample & hold voltage (V_{ref}) must be more than voltage of PV panel (V_{pv}). For example, shading over the PV panel occurs, causing V_{ref} to be more than V_{pv}, and switching at NMOS 3 gate to commence. Typically the greater the difference between V_{ref} and V_{pv}, the larger the duty cycle of the switching signal will be.

At $\approx$ 320 lux, the PV panel shows an open circuit voltage of about 1.36 V and V_{pv} voltage of about 0.3 V (Figure.13). At this lux level, the maximum power that the PV panel is able to produce is about 76 μW, which correspond to around 0.8 V and 0.1 mA on the PV and IV graphs. This maximum power point voltage is captured by the sample and hold circuit. When connected to rest of the circuit, the V_{pv} voltage drops to about 0.3 V, which corresponds to $\approx$ 40 μW. There is a further voltage drop of $\approx$ 0.11 V drop across the Schottky diode. Therefore the input voltage to the boost converter is around 200 mV.

The configuration of the differential op amp will influence the duty cycle to the gate of NMOS 3, which will in turn determine the output voltage of the boost converter. In an earlier configuration, the op amp has been configured to give an output voltage where V_{out} = 1/3

Fig. 13. Voltage across PV panel

Fig. 14. Voltage waveform at input of boost converter

[V(+) - V(-)]. V(+) is about 0.8 V, while V(-) is about 0.3 V. V_{out} of the differential op amp is about 0.167 V. When compared with the sawtooth waveform, duty cycle of around 30% is produced to NMOS 3. Using boost converter formulae, $V_{out} = V_{in}/(1-D)$, output voltage of converter is about 300 mV (200 mV / 0.7) when its input voltage is around 200 mV, as shown in Figures.14-16.

5.2 Power conversion efficiency of FEH system

At 320 lux, the PV panel produces $P_{pv} = V_{pv} * I_{pv} = 300mV * 0.11mA = 0.033mW$ when connected to rest of circuitry. At input of boost converter, P_{in} = V*I = 190 mV*0.1 mA = 19 μW. Difference in power between P_{pv} and Power at Boost converter input is due to the voltage drop across the Schottky diode after NMOS 1. At output, $P_{out} = V_{load} * I_o$ = 300 mV*36 μA = 10.8 μW. Efficiency of the boost converter, η = 10.8 μW/19 μW $\approx$ 60%.

At 320 lux, G = 320/120 $\approx$ 2.67 W/m^2.

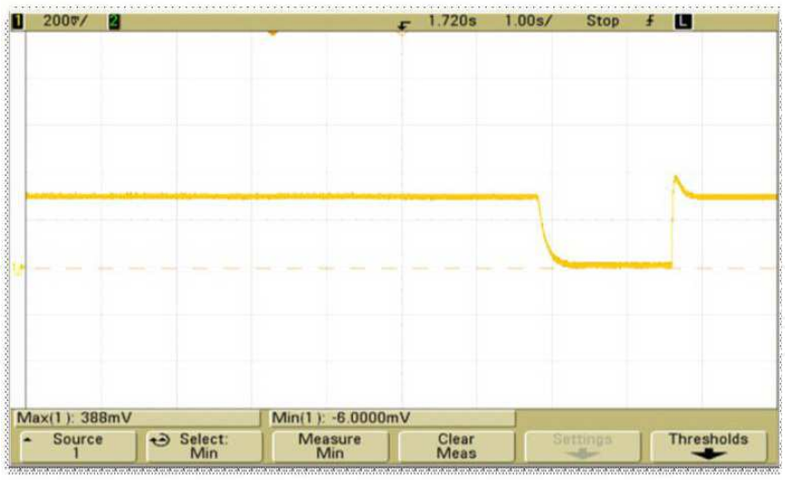

Fig. 15. Waveform at output load

Fig. 16. No switching at Gate of NMOS3 when V_{ref} is less than V_{pv}

Parameter	Unit	Value
Cross-section area	cm^2	7.2 x 5.9 = 42.48
OC voltage	V	1.46
SC current	µA	155
MPPT voltage	V	0.886
MPPT current	µA	86.3

Table 1. Technical Characteristic of PV Panel used

Efficiency of flexible PV panel:

$$\begin{aligned} \eta_{pv} &= \frac{P_{pv}}{G * A} * 100\% \\ &= [(0.886V * 86.3\mu A)/(2.67W/m^2 * 42.48cm^2)] * 100\% \\ &= 0.73\% \end{aligned} \tag{4}$$

At 400 lux, the maximum power that the PV panel is able to produce is about 130 μW, which correspond to around 1 V and 0.13 mA on the PV and IV graphs. At output of boost converter, current is about 40 μA. Over a 5 second period, total current accumulated is 200 μA.sec, which is able to fulfill the 0.2 mA needed by the end device for transmission in a 5 second period.

5.2.1 Power consumption study of discrete components within the fractional open circuit voltage approach control circuit

When using a 555-timer and op-amp inverter (MAX9077) to control the opening and closing for NMOS 1 and 2, the power consumption is shown in the next table.

	mA		Voltage (V), from Power Supply	Power (mW)	% of current consumed by
Total system current consumption	0.27		2.5	0.675	
CMOS 555 TIMER	0.121		2.5	0.3025	44.81%
MAX9077	0.0053	5.3uA	2.5	0.01325	1.96%
LTC6906	0.00984	9.84uA	2.5	0.0246	3.64%
LMC7215	0.0065	6.5uA	2.5	0.01625	2.41%
MAX4471 (2 Op Amps)	0.04	40uA	2.5	0.1	14.81%

Table 2. MPPT control circuit power consumption at 2.5V

From Table.2, both components (555-timer and MAX9077) take up $\approx$ 40 % of the total MPPT control circuit power consumption. We can decrease the total discrete components power consumption within the MPPT control circuit by using the RF transceiver's MCU to provide the timing pulse function to control NMOS 1 and 2.

5.2.2 Current limiter

A current limiter, LM334 National Semiconductor (2011) is added to protect the flexible battery from any massive drain due to possible surge in load. At 0.14mA limit, the flexible is able to take care of the quiescent current of the target board. If constant drawing of 0.14 mA from a fully charged 30 mAh flexible primary battery, calculated life expectancy of flexible battery will be: Duration = 30 [mA*hrs] / 0.14 [mA] $\approx$ 8.93 days

5.2.3 Voltage regulation

The voltage regulator, LTC3525-3.3 Linear Tech. (2011) is a compact, step-up DC-DC converters used to regulate the output voltage to the target board. The regulator has a V_{in} range of 0.5 V to 4.5 V, fixed output voltage of 3.3V and capable of delivering 60 mA at 3.3 V from a 1 V input. Quiescent current is an ultra-low 7 μA, maximizing battery life in portable applications. Its efficiency verse load current drawn is shown in Figure 17.

5.3 Application of hybrid FEH and storage for wearable wireless body sensor network

In the placement of the prototype, the flexible batteries and supercapacitor are flexible enough to bend along the contours of the human body, like on the forearm and shoulder.

Unlike flexible supercapacitor which has higher capacitance when twisted than any non-twisted supercapacitor Zyga (2011), flexible PV panel will see a further decrease in efficiency if bended as solar irradiance will decrease with less PV panel surface exposed directly to the light source (see Figure.20).

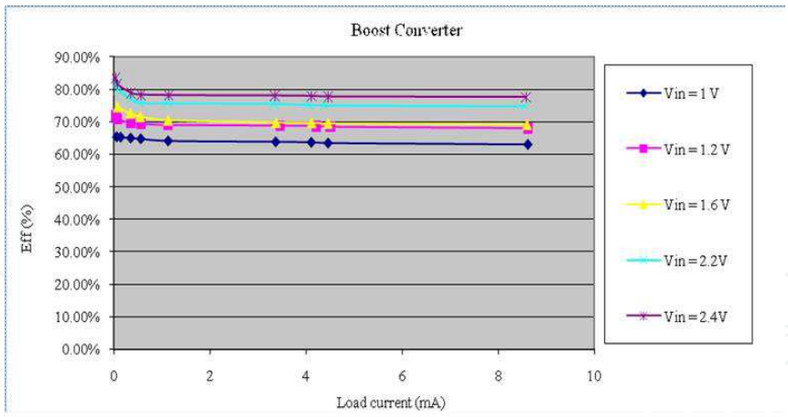

Fig. 17. Efficiency verse load current graph of boost converter

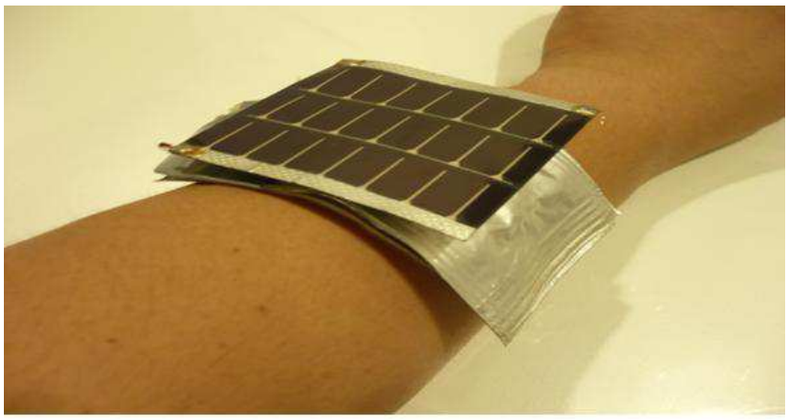

Fig. 18. Prototype placed and wrapped around the forearm

Fig. 19. Prototype placed at shoulder

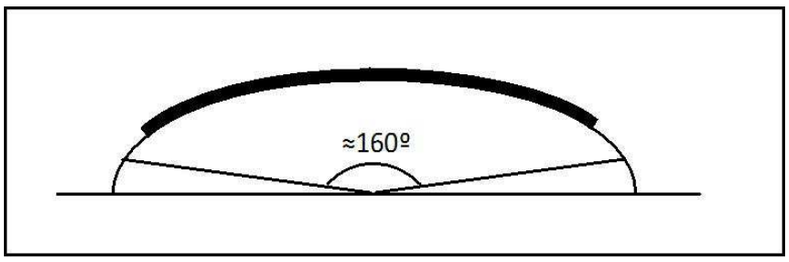

Fig. 20. Flexible PV panel placed on an arc with circular angle of 160ž

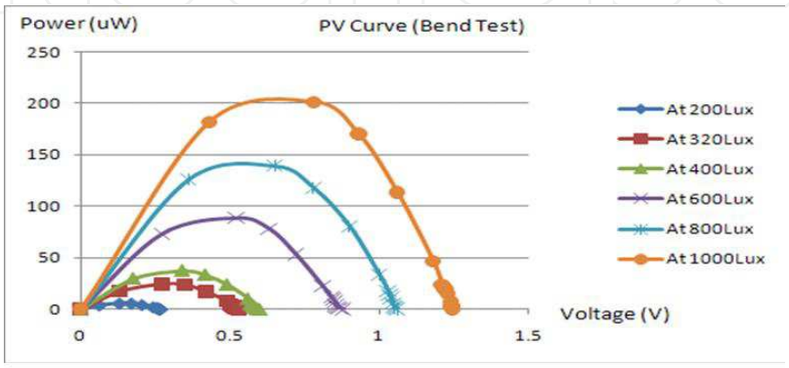

Fig. 21. PV Curves of PV panel at various Lux values when subjected to bending

From Figure.21, power produced dropped to about 1/3 of that from a flat panel. However as a starting platform, functional experiment is conducted with a flat prototype in a controlled environment.

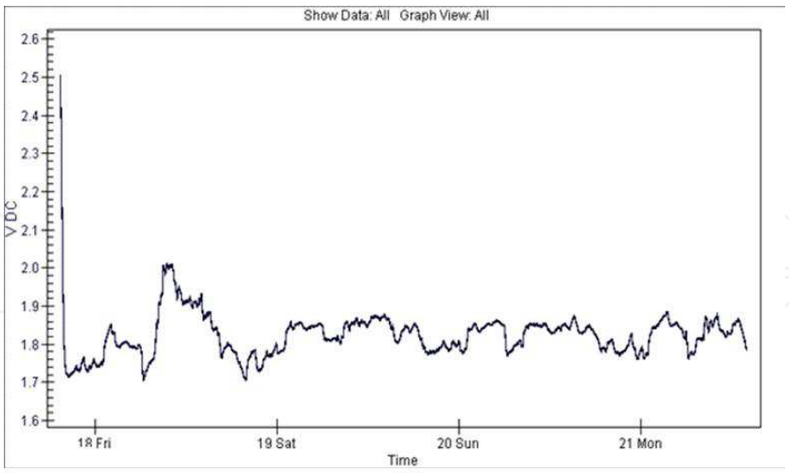

Fig. 22. Constant super capacitor voltage of around 1.7 V under a constant light source of 400 lux

Referring to Figure.22, it can be seen that the functionality experiment of prototype, under a constant light source of ≈ 400 lux, the system is self sustainable, powering the target board

and maintaining a super capacitor voltage of around 1.7 V. The experimental result verifies that the proposed hybrid flexible energy harvesting and storage system is able to sustain the operation of a wireless body sensor node connected in a network form.

6. Conclusions

Utilization of the PV harvesting prototypes together with its individual parts has been introduced. Under constant light intensity of 400 lux in a controlled environment, the prototype is able to operate in a self-sustaining mode, where the super capacitor voltage maintains at around 1.7 V. With its flexible attribute, it can be expanded to wearable, biomedical, constraint space applications and subsequent flexible design can be modified to incorporate other harvesting techniques.

7. References

United Nations, Department of Economic and Social Affairs, Population Division, "World Population Ageing: 1950-2050", >http://www.un.org/esa /population /publications/worldageing19502050/< assessed on 02-09-2011.

Harry K. Charles, Jr. and Russell P. Cain, "Ultra-thin, and Flexible Physiological Monitoring System", *IEEE Sensors Applications Symposium*, 2009

Philippe Jourand, Hans De Clercq, Rogier Corthout, Robert Puers, "Textile Integrated Breathing and ECG Monitoring System", *Proceedings of the Eurosensors XXIII conference, Procedia Chemistry 1*, pp.722-725, 2009.

D. Marculescu, R. Marculescu, S. Park and S. Jayaraman, "Ready to Ware", *IEEE Spectrum*, pp.28-32, 2003.

A.J. Wixted, D.V. Thiel, A.G. Hahn, C.J. Gore, D.B. Pyne and D.A. James, "Measurement of Energy Expenditure in Elite Athletes Using MEMS-Based Triaxial Accelerometers", *IEEE Sensors Journal*, vol.7, no.4, pp.481-488, 2007.

D.J. Cook and S. K. Das, "Wireless Sensor Networks - Smart Environments: Technologies, Protocols and Applications", *John Wiley*, New York, 2004.

Yen Kheng Tan, Sanjib Kumar Panda, "Review of Energy Harvesting Technologies for Sustainable Wireless Sensor Network", Sustainable Wireless Sensor Networks, *INTECH Publisher*, Chap 2, pp.15-43, 2010.

V. Raghunathan, A. Kansal, J. Hsu, J. Friedman and M. Srivastava, "Design Considerations for Solar Energy Harvesting Wireless Embedded Systems", *Fourth International Symposium on Information Processing in Sensor Networks Proceedings*, pp.457-462, 2005.

A. Hande, T. Polk, W. Walker, and D. Bhatia, "Indoor Solar Energy Harvesting for Sensor Network Router Nodes", Microprocess. Microsyst., vol.31, no.6, pp.420-432, 2007.

J.F. Randall, J. Jacot, "The Performance and Modelling of 8 Photovoltaic Materials under Variable Light Intensity and Spectra", *World Renewable Energy Conference VII Proceedings*, Cologne, Germany, 2002.

S. Roundy, P.K. Wright, J.M. Rabaey, "Energy Scavenging for Wireless Sensor Networks: with Special Focus on Vibrations". *Kluwer Academic Publishers*, 2004.

Adel Nasiri, Salaheddin A. Zabalawi, Goran Mandic, "Indoor Power Harvesting Using Photovoltaic Cells for Low-Power Applications", *IEEE Transactions on Industrial Electronics*, vol.56, no.11, 2009.

Robert Hahn, Herbert Reichl, "Batteries and Power Supplies for Wearable and Ubiquitous Computing", *Third International Symposium on Wearable Computers*, Digest of Papers, 1999.

Hiong Yap Gan, Cheng Hwee Chua, Soon Mei Chan and Boon Keng Lok, "Performance Characterization of Flexible Printed Supercapacitors", *11th Electronics Packaging Technology Conference*, 2009.

Jason Mcdonald, "Thin film battery technology and advanced batteries", >http://www.eg3.com/blog/20090420.htm< assessed on 02-09-2011.

P.A. Barbic, L. Binder, S. Voss, F. Hofer and W. Grogger, "Thin-Film Zinc/Manganese Dioxide Electrodes based on Microporous Polymer Foils", *Journal of Power Sources*, vol.79, issue.2, pp.271-276, 1999.

Jenny Nelson, "The Physics of Solar Cells", *Imperial College Press*, >http://www.worldscibooks.com/ physics/p276.htm< assessed on 02-09-2011.

Ali Naci Celik, Nasir Acikgoz, "Modelling and Experimental Verification of the operating current of mono-crystalline photovoltaic modules using four- and five-parameter models", *Applied Energy*, vol.84, issue.1, pp.1-15, 2007.

Sundance Solar, "Small Solar Panels for science fair projects, experiments and prototypes", >http://store.sundancesolar.com/smalsolpanfo.html< assessed on 02-09-2011.

Grace Wee, Oscar Larsson, Madhavi Srinivasan, Magnus Berggren, Xavier Crispin, Subodh Mhaisalkar, "Effect of the Ionic Conductivity on the Performance of Polyelectrolyte-Based Supercapacitors", *Advanced Functional Materials*, pp.4344-4350, 2010.

V. Salas, E. Olit'as, A. Barrado, A. Lat'zaro, "Review of the Maximum Power Point Tracking Algorithms for Stand-alone Photovoltaic Systems", *Solar Energy Materials & Solar Cells 90 (2006)*, pp.1555-1578, 2005.

M.A.S. Masoum, H. Dehbonei, "Design Construction and Testing of a Voltage-based Maximum Power Point Tracker for Small Satellite Power Supply", *Proceedings of 13th annual AIAA/USU Conference on Small Satellite*, 1999.

Jawad Ahmad, "A Fractional Open Circuit Voltage Based Maximum Power Point Tracker for Photovoltaic Arrays", *2nd International Conference on Software Technology and Engineering (ICSTE)*, 2010.

Texas Instruments, eZ430-RF2500 Development Tool, Datasheet.

Texas Instruments, eZ430-RF2500 Development Tool, Application Notes.

National Semiconductor, LM334, Datasheet.

Linear Technology, LTC3525-3.3, Datasheet.

Lisa Zyga, "Paper-thin supercapacitor has higher capacitance when twisted than any non-twisted supercapacitor", >http://www.physorg.com/news204265367.html< assessed on 02-09-2011.

Q. Zhang, P. Feng, Z.Q. Geng, X.Z. Yan, N.J. Wu, "A 2.4-GHz energy-efficient transmitter for wireless medical applications", *IEEE Transactions on Biomedical Circuits and Systems*, vol.5, no.1, pp.39-47, 2011.

O. Omeni, Alan C.W. Wong, Alison J. Burdett, C. Toumazou, "Energy efficient medium access protocol for wireless medical body area sensor networks", *IEEE Transactions on Biomedical Circuits and Systems*, vol.2, no.4, pp.251-259, 2008.

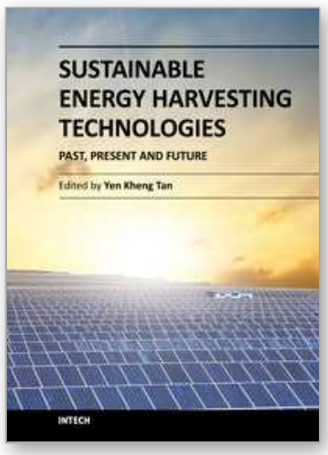

Sustainable Energy Harvesting Technologies - Past, Present and Future

Edited by Dr. Yen Kheng Tan

ISBN 978-953-307-438-2
Hard cover, 256 pages
Publisher InTech
Published online 22, December, 2011
Published in print edition December, 2011

In the early 21st century, research and development of sustainable energy harvesting (EH) technologies have started. Since then, many EH technologies have evolved, advanced and even been successfully developed into hardware prototypes for sustaining the operational lifetime of low?power electronic devices like mobile gadgets, smart wireless sensor networks, etc. Energy harvesting is a technology that harvests freely available renewable energy from the ambient environment to recharge or put used energy back into the energy storage devices without the hassle of disrupting or even discontinuing the normal operation of the specific application. With the prior knowledge and experience developed over a decade ago, progress of sustainable EH technologies research is still intact and ongoing. EH technologies are starting to mature and strong synergies are formulating with dedicate application areas. To move forward, now would be a good time to setup a review and brainstorm session to evaluate the past, investigate and think through the present and understand and plan for the future sustainable energy harvesting technologies.

How to reference

In order to correctly reference this scholarly work, feel free to copy and paste the following:

Yen Kheng Tan and Wee Song Koh (2011). Wearable Energy Harvesting System for Powering Wireless Devices, Sustainable Energy Harvesting Technologies - Past, Present and Future, Dr. Yen Kheng Tan (Ed.), ISBN: 978-953-307-438-2, InTech, Available from: http://www.intechopen.com/books/sustainable-energy-harvesting-technologies-past-present-and-future/wearable-energy-harvesting-system-for-powering-wireless-devices

INTECH
open science | open minds

InTech Europe
University Campus STeP Ri
Slavka Krautzeka 83/A
51000 Rijeka, Croatia
Phone: +385 (51) 770 447
Fax: +385 (51) 686 166
www.intechopen.com

InTech China
Unit 405, Office Block, Hotel Equatorial Shanghai
No.65, Yan An Road (West), Shanghai, 200040, China
中国上海市延安西路65号上海国际贵都大饭店办公楼405单元
Phone: +86-21-62489820
Fax: +86-21-62489821

© 2011 The Author(s). Licensee IntechOpen. This is an open access article distributed under the terms of the Creative Commons Attribution 3.0 License, which permits unrestricted use, distribution, and reproduction in any medium, provided the original work is properly cited.

IntechOpen

IntechOpen